

He also thanks Professor S. Hosoya and Mr T. Fukamachi for the measurement of TDS by X-ray diffraction. For the calculation part of the work, he is indebted to Professor K. Molière for the generous hospitality of his department and also thanks the Max-Planck-Gesellschaft and the Alexander von Humboldt-Stiftung for financial support.

References

- CUNDY, S. L., HOWIE, A. & VALDRÉ, U. (1969) *Phil. Mag.* **20**, 147–163.
- FUJIMOTO, F. (1959). *J. Phys. Soc. Japan*, **14**, 1558–1568.
- GEVERS, R., BLANK, H. & AMELINCKX, A. (1966). *Phys. Stat. Sol.* **13**, 449–465.
- GOODMAN, P. & LEHMPFUHL, G. (1967). *Acta Cryst.* **22**, 14–24.
- KOHRA, K. & WATANABE, H. (1961). *J. Phys. Soc. Japan*, **16**, 580–581.
- NIEHRS, H. (1959). *Z. Naturforsch.* **14A**, 504–511.
- POGANY, A. P. & TURNER, P. S. (1968). *Acta Cryst.* **A24**, 103–109.
- TAKAGI, S. (1958). *J. Phys. Soc. Japan*, **13**, 287–296.
- TANAKA, M. & HONJO, G. (1964). *J. Phys. Soc. Japan*, **19**, 954–970.
- TANAKA, M. & HONJO, G. (1966). *Sixth International Congress for Electron Microscopy, Kyoto*, pp. 83–84.
- TANAKA, M. & HONJO, G. (1970). *Seventh International Congress for Electron Microscopy, Grenoble*, pp. 55–56.
- TANAKA, M. & LEHMPFUHL, G. (1972). *Jap. J. Appl. Phys.* **11**, 1755–1756.
- TANAKA, M., YATSUHASHI, T. & HONJO, G. (1970). *J. Phys. Soc. Japan*, **28**, Suppl., 386–388.
- WICKS, B. J. & LEWIS, M. H. (1968). *Phys. Stat. Sol.* **26**, 571–576.

Acta Cryst. (1975). **A31**, 63

Structure Analysis of the γ Phase in the Vanadium Oxide System by Electron Diffraction Studies

BY B. ANDERSSON

Department of Physics, University of Oslo, Oslo, Norway

(Received 3 July 1974; accepted 7 August 1974)

The structure of the γ phase ($\text{VO}_{0.53}$) has been analysed by electron diffraction from single crystals. Intensities in the spot patterns were compared with calculations based on dynamical theory for scattering of electrons for ideal crystals. It was found necessary to include corrections due to bending of the crystal. The structure can be regarded as a rock-salt type with oxygen vacancies or as body-centred cubic with interstitial oxygen. Possible ways of distributing oxygen on the available sites have been tried. The only structure models which produce a reasonable fit have oxygen atoms arranged in close-packed rows with the vanadium atoms displaced to give V–O and V–V distances in accordance with the corresponding distance in V and VO. Diffuse scattering indicating further ordering of vacancies has been observed.

1. Introduction

In the lower part of the composition range in the V–O system a phase, called γ in the nomenclature given by J. Stringer (1965), appears at the approximate composition $\text{VO}_{0.5}$. Its existence was first proposed by Rostoker & Yamamoto (1955) and was confirmed by a phase analysis by Westman & Nordmark (1960), based on X-ray powder diffraction. From a comparison with the neighbouring phases they suggested the structure to be a transition between the structure of the β phase ($\text{VO}_{0.3}$) and the monoxide. Later, Westman (1963) proposed a monoclinic unit cell for indexing the line patterns. The composition range around $\text{VO}_{0.5}$ has also been studied by electron microscopy combined with X-ray powder diffraction by Cambini, Pellegrini & Amelinckx (1971). They reported a phase at the same composition but proposed a different monoclinic unit

cell. Structure analysis of the γ phase has not been carried out so far.

Such an analysis is of interest also for the understanding of the nature and ordering of defects in the neighbouring suboxide and monoxide regions. A main aim of the present investigation, in which a structure analysis has been carried out by means of electron diffraction, has been to gain further insight into the defect structure in the lower part of the monoxide region. Since the single crystals are small, neutron or X-ray single-crystal methods could not be applied; neither could powder methods because the lines contain contributions from several non-equivalent reflexions.

The ease with which single-crystal patterns can be obtained by electron diffraction techniques, combined with the imaging of the diffracting regions, leads to easy determination of the unit cell and also of possible space groups. It is mainly this powerful side of the

technique that has been applied in structure analysis, particularly to various forms of superstructures.

Electron diffraction is unfortunately not so well suited for obtaining information about atomic arrangements within the unit cell. Owing to dynamical effects, the intensities will depend on a large number of structure factors as well as on the detailed diffraction conditions and thickness. In addition imperfections like deformations, foreign atoms and nonperiodic atomic distribution will affect the intensities.

Electron diffraction should in principle yield more structure information than X-ray diffraction since intensities depend not only on the size of the structure factors but also on relative phases. The dynamical effects can be utilized for accurate determination of inner strong reflexions. The methods require perfect crystals and some also require special crystal geometry. If these requirements can be met, the methods are well suited to the refinement of structures. For a solution, however, a larger number of structure factors must be known.

The difficulties arising from dynamical scattering can, to a certain extent, be avoided by keeping to near-kinematical conditions. A further advantage can be gained by having a statistical distribution of orientations. Arc or ring patterns from polycrystalline materials with small effective single-crystal size have been used to solve a number of structures (Vainshtein, 1964). The intensities in the spot patterns from mosaic crystals have been related to the structure factor by the simple formula

$$F_{hkl} = \sqrt{I_{hkl}/d}$$

where d is the interplanar distance. It is then assumed that only strong reflexions need dynamical correction (Harada & Kitamura, 1964; Udalova & Pinsker, 1964). This formula has also been applied to the study of spot patterns from clay minerals (Drits, Organova & Dmitrik, 1972) which have large single crystals but which, can be prepared in very thin samples.

Outside the limited range of materials suited to these methods one has to deal with dynamical interactions. In the present investigation it was not possible to obtain the required crystal size or the geometry necessary for applying dynamical or near-kinematical methods. Spot patterns were obtained from areas of varying thickness and orientations; a morphology which may be typical for a wide range of inorganic materials. Since the intensities showed good reproducibility and had a very marked change from reflexion to reflexion, it appeared that much structure information was present in the intensity data. A further aim was therefore to explore the possibilities of making a structure analysis based upon the spot patterns from such crystals.

2. Experimental

Specimens of the desired composition were prepared by arc melting together weighed amounts of vanadium

metal and the sesquioxide V_2O_3 , followed by a heat treatment in evacuated silica tubes for 2 weeks at 700°C. Foils for examination in the electron microscope were thinned electrolytically and finally etched (Andersson & Gjønnes, 1970).

X-ray powder patterns were recorded with a Guinier camera and Cu $K\alpha$ radiation with KCl as the internal standard.

3. Preliminary structure analysis

Reciprocal lattice

The Bravais lattice and the approximate cell parameters were determined from single-crystal electron diffraction patterns. A refinement was based on X-ray powder data given by Westman & Nordmark (1960). The results turned out to be close to those of Cambini *et al.* (1971) with the same monoclinic C -centred lattice and nearly the same values for the parameters. The authors have therefore doubtlessly studied the same phase.

The transformed results of Westman (1963) from $VO_{0.53}$ together with those of Cambini *et al.* (1971) (in parentheses) are $a=9.50$ (9.52), $b=2.926$ (2.95), $c=7.732$ Å (7.77 Å), $\beta=90.38^\circ$ (90.67°).

The transformation from the slightly monoclinically deformed tetragonal subcell (indexed t) with $a_t \approx 2.93$ Å and $c_t \approx 3.55$ Å used by Westman (1963) to the unit cell of the γ -phase is

$$\begin{aligned} a &= 3a_t + c_t \\ b &= b_t \\ c &= 2c_t + a_t \\ \beta &\approx \beta_t. \end{aligned}$$

The only possible extinction rule in the Bravais lattice is $h0l: l \neq 2n (h \neq 2n)$; $00l: (l \neq 2n)$. No extinction was observed in the (010) plane. If the above rule is operating, reflexions such as 001, 003 *etc.* can occur neither from the central beam nor from any of the present reflexions. The possible space groups, having no symmetry extinctions, are then $C2, Cm, C2/m$.

The last two space groups include a mirror plane parallel to (010). If atoms are positioned in a manner similar to f.c.c. or b.c.c., they must be in that plane. To allow for a displacement out of the plane, without there being a mirror atom, the space group $C2$ was chosen.

Composition

The single-phase region of the γ structure is apparently quite narrow since traces of neighbouring phases have always been found. The composition $VO_{0.53}$ was proposed by Westman & Nordmark (1960). The unit cell should contain 13 vanadium and 7 oxygen atoms to comply with the observed average density $d=5.9$ g cm^{-3} . The closest ideal composition is $V_{14}O_8$ ($VO_{0.57}$) since an odd number of atoms is not allowed. The density will, however, be $d=6.2$ g cm^{-3} . Owing to the ambiguity, the following compositions have been considered: $V_{14}O_8, V_{14}O_6, V_{12}O_8$ and $V_{12}O_6$.



Fig. 2. $(1\bar{1}0)$ reciprocal-lattice plane which corresponds to $\{112\}$ or $\{110\}$ in NaCl and b.c.c. types of structures respectively.

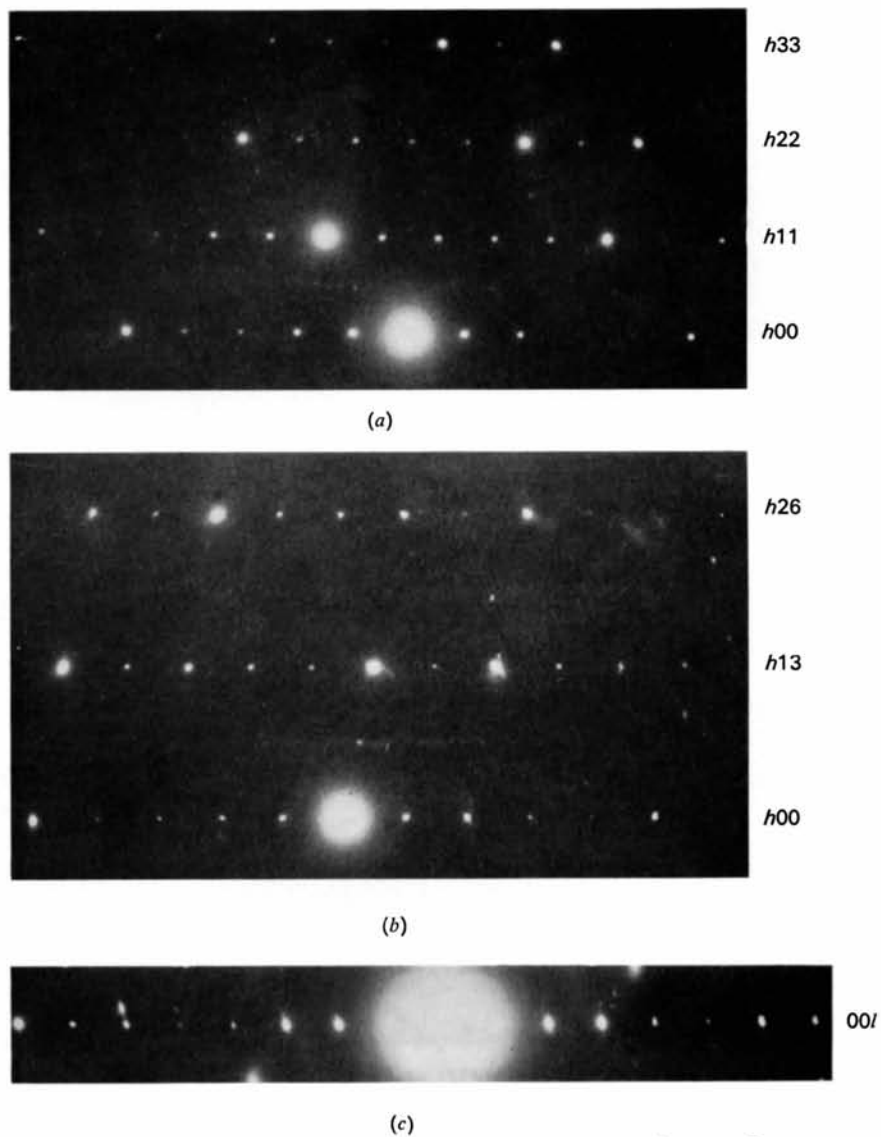


Fig. 3. The lattice planes used in the electron-diffraction calculations. (a) $(0\bar{1}1)$, (b) $(0\bar{3}1)$, and (c) the $00l$ line.

Structure models

Considerations of some general properties of the V–O system served as a starting point for the structure analysis. Interstitial atoms like carbon, nitrogen and oxygen normally occur in the octahedral interstices in transition metals with a body-centred structure. These belong to three sets of sites (Fig. 1) called x, y, z . As the interstitial fraction increases, one of the sets, say z , is preferred and the corresponding c axis elongated. This tetragonal distortion is similar to the Bain deformation introduced in the description of iron–carbon martensite. The tetragonality increases with concentration of interstitial atoms until all the sites within a set are occupied. The resulting NaCl structure can be referred to a body-centred tetragonal subcell with $c/a = \sqrt{2}$.

In the V–O system the martensitic suboxide VO_x , the β and γ phases form a succession of phases between the body-centred V and rock-salt type VO in which the c axis of the b.c. tetragonal subcell continuously increases from V to VO. Thus the oxygen atoms in the γ phase are expected to enter one set of octahedral sites as referred to this subcell.

It is known, especially from studies of Fe–C martensite, that the b.c.t. cell represents an average cell. The interstitials will in fact force the two neighbouring metal atoms apart in the z direction whereas the metal atoms relax over the empty z sites.

The V atoms will have a dominating effect on the diffraction pattern owing to the larger scattering factor and concentration. From lattice planes containing subcell reflexions (Fig. 2) it is observed that the intensities of superlattice reflexions are stronger in the vicinity of subcell reflexions, a feature typical in the displacement type of ordering (Guinier, 1963). Furthermore, the neighbours of subcell reflexions are relatively stronger when the plane normal is closer to the z direction. This behaviour indicates that the displacements are mainly along the z direction, confirming the suppositions made from structural considerations.

The structure can thus be formed by b.c.c. vanadium with oxygen atoms in octahedral sites forcing vanadium

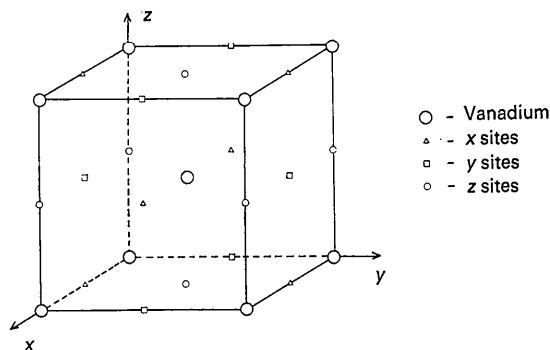


Fig. 1. A b.c.c. unit cell showing the three sets of octahedral sites.

atoms apart or alternatively, by the NaCl type of VO having octahedral oxygen vacancies with V atoms relaxed. It is advantageous to describe the structure in terms of ideal subcell positions. The actual V atoms will be displaced to form realistic V–V and V–O distances. Such a reference structure will contain 14 metal and oxygen sites distributed on one twofold and three fourfold positions. The coordinates of each position, numbered from 1 to 4, are the following:

V(1) in 2(a)	0	0	0
V(2) in 4(c)	$\frac{2}{3}$	0	$\frac{1}{3}$
V(3) in 4(c)	$\frac{4}{3}$	0	$\frac{2}{3}$
V(4) in 4(c)	$\frac{8}{3}$	0	$\frac{5}{3}$
O(1) in 2(b)	0	$\frac{1}{2}$	$\frac{1}{2}$
O(2) in 4(c)	$\frac{1}{3}$	$\frac{1}{2}$	$\frac{1}{14}$
O(3) in 4(c)	$\frac{2}{3}$	$\frac{1}{2}$	$\frac{3}{14}$
O(4) in 4(c)	$\frac{4}{3}$	$\frac{1}{2}$	$\frac{5}{14}$

All possible combinations for the different compositions are listed in Table 1 together with the number of vacancy pairs in a unit cell along the $[100]_t$ and $[001]_t$ directions.

Table 1. Possible atom combinations for the compositions

Structure model	Com-position	Vacant O positions	$[100]_t$ pairs	$[001]_t$ pairs
1	V_{14}O_8	O(1) + O(4)	4	0
2		O(1) + O(2)	0	4
3		O(1) + O(3)	0	0
7	V_{14}O_6	O(2) + O(3)	6	2
8		O(3) + O(4)	4	6
9		O(2) + O(4)	0	4

The structure models 4–6 for V_{12}O_8 and 10–12 for V_{12}O_6 are the same as 1–3 and 7–9 respectively with V(1) vacant in addition. The models are of three types: one having vacancy rows along $[100]_t$, a second along $[001]_t$ and a third having isolated or pairs of vacancies. The models for each composition are listed in the same sequence in the table.

X-ray work

The intensities of only six lines could be measured in the X-ray powder diffraction patterns. These lines had contributions from several non-equivalent reflexions and were insufficient as a basis for a structure proposal.

The intensities could, however, serve as a guide to the value of the displacements. In each of the possible models the V atoms were displaced, governed by a single parameter, towards the vacancies until a minimum was reached in the reliability parameter R . The values obtained ranged from 0.07 to 0.14. The position of each metal site was then varied in the (010) plane to a new lower minimum which in this case ranged from 0.05 to 0.08. Both sets of positions were used in the subsequent calculations.

4. Electron diffraction studies

The aim of the electron diffraction studies was to exploit the experimental spot-pattern intensities for distinguishing between the different models based on elements outlined in the previous section; *i.e.* ordering of oxygen vacancies referred to the NaCl-type of structure, and related atomic displacements around the vacancies.

Diffraction patterns from areas near the edges of specimens correspond to thicknesses ranging from 0 to 1000 Å. The crystals were irregular and no special thickness dominated. The degree of bending could not be judged from the extinction contour owing to the varying thickness. The diffraction patterns obtained from thick crystals showed only broad low-order Kikuchi-lines and the bending within the area contributing to the pattern was thence estimated to be $\frac{1}{20} - \frac{1}{10}^\circ$.

The spot intensities in the patterns show many signs of being subject to dynamical interactions. Referring to Fig. 3, one may expect the intensities of for instance $\bar{2}22$, 422 , 226 and 626 to receive appreciable contributions from 'umweganregung'. Comparing the single $00l$ line, particularly the 007 reflexion [Fig. 3(c)] with the same line in the lattice plane $(1\bar{1}0)$ (Fig. 2), it is evident that the latter is considerably changed by the presence of other reflexions. In curves like the one reproduced in Fig. 4, the dynamical interactions show up in a slower decline in intensity with diffraction angle than that expected from kinematical theory. The interpretation of the intensity must therefore be based on dynamical theory and include the effects of varying thickness and bending.

The intensities in the dynamical case are not simply related to the structure factors. Earlier dynamical calculations in highly symmetrical planes of the superstructure $V_{52}O_{64}$ of the cubic monoxide demonstrated that intensities of superlattice reflexions are, in a way, averaged by the numerous strong interactions. The intensities were found to be on the same level despite large differences in structure factors. The same effect can be seen in lattice plane $(1\bar{1}0)$ (Fig. 2). Owing to strong subcell reflexions, the neighbouring reflexions tend to have relatively the same variation. As a result the pattern will mainly carry information about the average position within the subcell and not of the interesting longer correlations. The choice of reciprocal-lattice planes is therefore of major importance. Care must be taken to ensure that the intensities are sensitive to the structure elements under considerations.

The chosen planes were $(0\bar{3}1)$ and $(0\bar{1}1)$; both involved 55 beams together with the $00l$ line of reflexions with 17 beams. Only the first plane contains one pair of very strong subcell reflexions. Because of the absence of the very strong interactions, a large range of structure factors will result in a corresponding large range of intensities (Fig. 3).

Dynamical calculations are usually referred to a

fixed thickness or given as an average over all thicknesses up to infinity. Neither of the two procedures can be strictly correct here. The specimen thickness varies over a range but an averaging procedure including infinity will only be meaningful if the intensity variations are periodic with thickness, as is the case at symmetrical incidence. In order to explore the thickness dependence, the intensity was calculated in the range 100–2000 Å for a representative structure model. It turned out that the intensities oscillate strongly with thickness, roughly about the average corresponding to infinite thickness. An average performed over a thickness range of 300 Å or more was found to be an adequate approximation. Several such averages were applied.

When intensities were calculated for one particular orientation, large systematic deviations were experienced [Fig. 4(b)]. Inner reflexions appeared with too large values, the outer ones being too small. The bending of crystal planes has an effect similar to that of a mosaic nature of the crystal. The relation $I \propto F^2/d$ in the kinematical case seems to be valid for very thin crystals (Driets *et al.*, 1972), but the correcting factor $1/d$ did not fit well in the present case. This is not surprising since the intensity is affected in a very complicated way by the strength and relative phases of all the beams present. Accurate calculations of the intensity should be performed as an average over the range of orientations

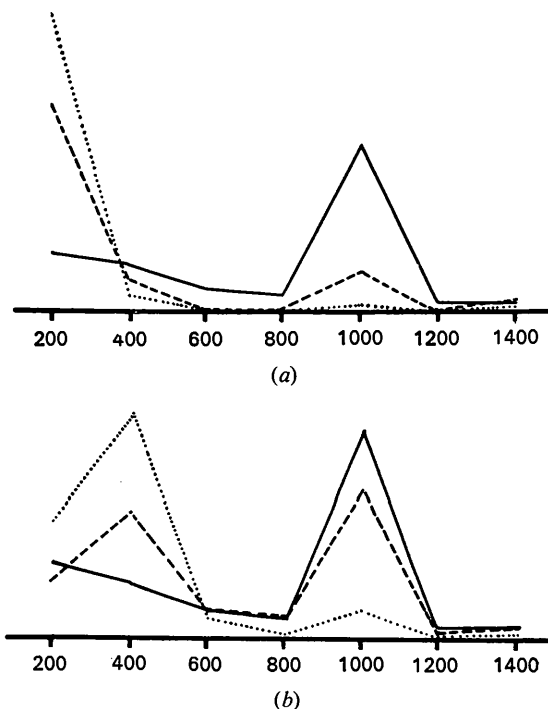


Fig. 4. Observed intensities (full lines) compared with intensities calculated (a) by kinematical theory and (b) by dynamical theory. Dotted lines represent the uncorrected intensities and broken lines those corrected (a) by $1/d_{hkl}$ and (b) by formula (1).

present. The calculations will, however, be extensive, owing to the large number of orientations and also because the range of orientation is not known but will have to be adjusted.

Instead of such extensive calculations we have attempted an approximate correction to the intensities calculated for an ideal crystal of average orientation. As an expression for the intensity of a reflexion g the form

$$I_g = I_g(\bar{s}_g) \cdot H(\bar{s}_g, b_g),$$

where \bar{s}_g is the excitation error* corresponding to the average orientation, b_g is a parameter for the width of the g reflexion, was assumed. H is the correcting function. To have the expression in the proposed form it is assumed that the shape of all the reflexions is the same and also that the incident beam is near the zone axis.

The function H can be derived by making suppositions about shape and orientation distribution. A few attempts were made but an empirical procedure was preferred as the results were better.

The form of H was found experimentally by making graphs of the ratio between the observed intensity and the calculated $I_g(\bar{s}_g)$ against \bar{s}_g . In a graph where one takes the logarithm of the logarithm of the ratio, an approximately linear correspondence with \bar{s}_g was found, increasing up to $\bar{s}_g = 0.9 \text{ \AA}^{-2}$ and then slowly decreasing (Fig. 5). I_g can thus be described by

$$I_g \propto I_g(\bar{s}_g) \cdot \exp \{ \exp [K \cdot |\bar{s}_g|] \} \quad (1)$$

where $K = 1.67$ for $|\bar{s}_g| < 0.9 \text{ \AA}^{-2}$ and for $|\bar{s}_g| > 0.9$ the exponent $K \cdot |\bar{s}_g|$ is put equal to 1.5.

The dependence on width has been disregarded in this derivation but manifests itself as deviations, especially for weak reflexions. Since these are narrower, H should increase more steeply. As can be seen from the graph this is the case. The effect is so well defined that it has not been found necessary to make corrections in the intermediate calculations. In the final calculations

* The factor $2k$ is absorbed in s_g .

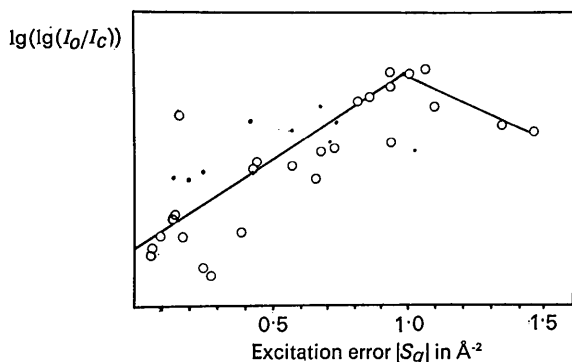


Fig. 5. The logarithm of the logarithm of the ratio between observed and dynamical calculated intensities as a function of excitation error. Open circles indicate strong reflexions and dots weak ones.

I_g itself has been used as the parameter for the width. The calculated intensity should be reduced for larger intensity values and enhanced appreciably for small values. The correction may be reminiscent of the Blackman correction to kinematically calculated intensities to be used when dynamical effects are encountered. Although the reason for correction is different, the same form is chosen for simplicity. The factor will be I_g^{-t} , and as a result the corrected intensity values can be written

$$I_g \propto \{ I_g(\bar{s}_g) \cdot \exp [\exp (K \cdot |\bar{s}_g|)] \}^{1-t} \quad (2)$$

where $t \approx 0.4$ is found to give the best fit.

When different lines of reflexions were compared, it was evident that the corrections were insufficient, probably owing to errors in the average orientation. Each line was therefore normalized separately.

5. Electron-diffraction calculations

The calculations of the intensities in the selected planes were based on the two sets of atomic positions derived from X-ray intensities for all 12 models. At first, the calculations were performed for all models without corrections, using symmetrical orientation. A refinement on the orientation in each plane was carried out on one of the best models to find the average orientation. Special attention was paid to the ratio between the intensities of g and $-g$ reflexions which were expected to be little affected by bending. The intensities were then calculated using these average orientations and with bending corrections applied.

The results for each model were compared with observed intensities. As an example the results for the $h22$ line are presented in Fig. 6. Only the set resulting in the best fit is shown. It became evident that only models belonging to the first structure type (shown with full lines) give a reasonable fit when all lines of reflexions are taken into consideration. The models 2, 5, 7 and 10 of the second type (shown with dotted lines) seem to be particularly unfavourable configurations. The disagreement is serious even for strong superlattice reflexions.

All models except 1, 4, 7, and 10 were consequently left out owing to the poor fit. In the subsequent calculations the positions in the four models were varied separately and different thickness averages made. The purpose of the refinement was to distinguish between the four models.

An average over all thicknesses was best suited for the models in the $(0\bar{3}1)$ plane and $00l$ line and an average around 500 \AA in the $(0\bar{1}1)$ plane. Model 1 ($V_{14}O_8$) could be refined to the best fit. The R index for the intensities was about 5–10% larger and in addition a few more unreasonable values resulted for the other three models. Whether this difference is sufficient reason for excluding or not excluding the models or is, however, not clear, owing to the inaccuracies of the electron diffraction method and also because a better fit may be

attained through more extensive and general variation of atomic positions. But besides the better fit the composition is closest to the experimentally determined value, and model 1 is therefore preferred. The positions in the proposed structure shown in Fig. 8 are:

V(1)	0	0	0
V(2)	0.274	0	0.179
V(3)	0.561	0	0.316
V(4)	0.845	0	0.463
O(2)	0.173	0.5	0.071
O(3)	0.429	0.5	0.214

The results are shown in Fig. 7 for the central line and the lines on one side in the patterns. The R value for the intensities in the two lattice planes was about 0.34. To obtain the R value on the same level as for structure factors, the square roots of the intensities can be used. The R value will then be 0.15.

6. Discussion

The main advantage of the electron-diffraction method as a tool in structure studies may be the ease with which the unit cell and systematic extinctions can be determined in systems where the crystals are very small. In many cases this has led to an adequate structure analysis, sometimes through combination with X-ray powder work.

The present study is that of a structure problem when this combination is not sufficient and when the simplifying assumption of kinematical or near-kinematical scattering conditions cannot be made. In order to determine the atomic arrangement, we therefore had to depend upon analysis of spot-pattern intensities under dynamical scattering conditions since other methods failed. The implication of such a procedure is, of course, that it does take multiple-beam interactions into account, especially for reflexions which are influenced by 'umweganregung'. The preliminary studies of the spot-pattern intensities showed that this is essential since these superstructure reflexions are indeed subject to 'umweganregung'.

The application of dynamical theory to ordinary, non-perfect crystals like the present one, calls for simplifying approximations. Since orientation and thickness are the dominating non-structural factors determining the intensities, good approximations to the distributions will certainly result in reliable values. The large increase in calculation time which is necessary to form averages and make adjustments appeared not to be justified. We have rather aimed at approximate corrections which would not increase the complexity of the calculations and still be adequate for determination of the broad features of the atomic arrangements.

The corrections were derived in an empirical way and the functional form may not carry any information about actual relations to the pertinent parameters describing orientation and thickness, although the resemblance of $H(\bar{s}_g)$ to the function $\exp |C|\bar{s}_g|^2|$ can be

taken as indication of a near Gaussian distribution of orientation.

The selected spot patterns proved to be sensitive to the type of ordering and most of the models could, therefore, be excluded as impossible on the basis of the patterns. Determining the correct model from four closely related ones is more uncertain with the present method. This is partly because the somewhat better fit may not be significant and partly because further variation of positions may lead to a better fit.

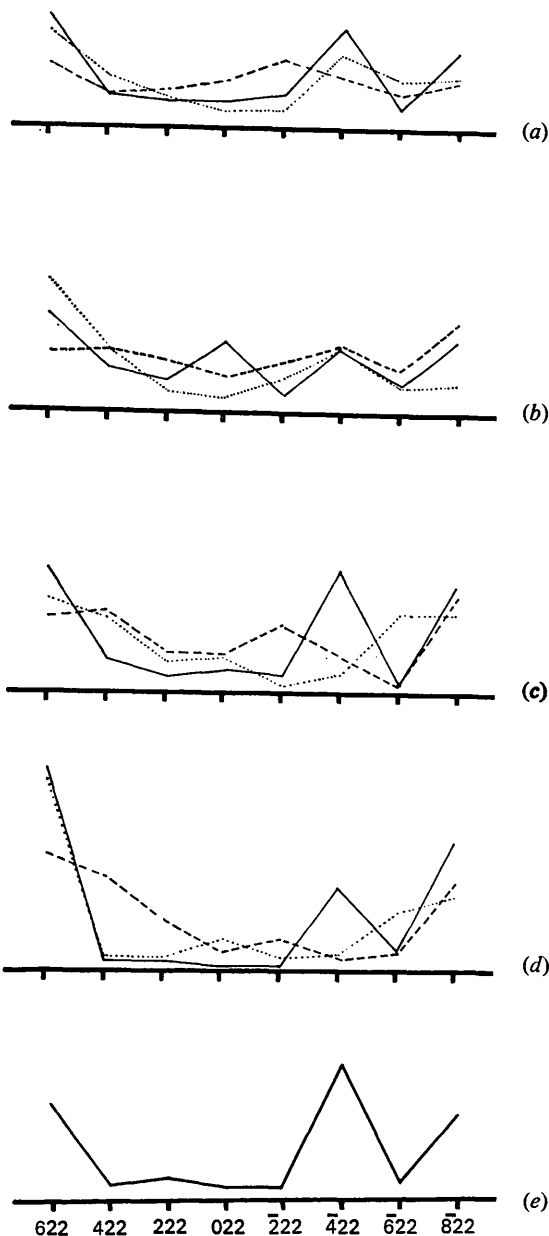


Fig. 6. Intensities in the $h22$ row of reflexions calculated for all models 1-12. (a) $V_{14}O_8$, (b) $V_{12}O_8$, (c) $V_{14}O_6$, (d) $V_{12}O_6$ and (e) the observed intensities. Full, broken and dotted lines correspond to the first, second and third structure types given in Table 1.

All models leading to reasonable fits were of the first type (Table 1) with vacancies gathered in close-packed rows. The models with composition $V_{14}O_8$ and $V_{12}O_8$ contain groups of three vacancies. In $V_{14}O_6$ and $V_{12}O_6$ one more vacancy is added. The neighbours of the vacancies form local vanadium-metal configurations, and the environment of the oxygen adopts a local monoxide configuration (Fig. 8). The structure can therefore be considered as composed of alternating layers of V and VO in the [001] or [113] direction indexed for a NaCl-type unit cell.

Even in the oxygen-deficient region of monoxide the fraction of oxygen vacancies is very high, about 30–20%. Diffraction patterns from samples in this region show strong diffuse scattering forming complex pat-

terns which indicate short-range ordering of defects over distances as large as $\sim 30 \text{ \AA}$ (Andersson, Gjønnnes & Taftø, 1972). It is of major interest to see if the favourable configuration typical of the γ phase is preserved also in the monoxide region. A similar feature is observed in the oxygen-rich part where the defect cluster of $V_{52}O_{64}$ is also present in the monoxide region (Andersson *et al.*, 1974). Work is, therefore, in progress to interpret the diffuse patterns in terms of vacancy rows or layers with corresponding displacements of vanadium atoms.

The appearance of additional scattering in diffuse bands in the [100] direction halfway between rows of reflexions (Fig. 3) indicates, together with the discrepancy in density, that the actual structure under investi-

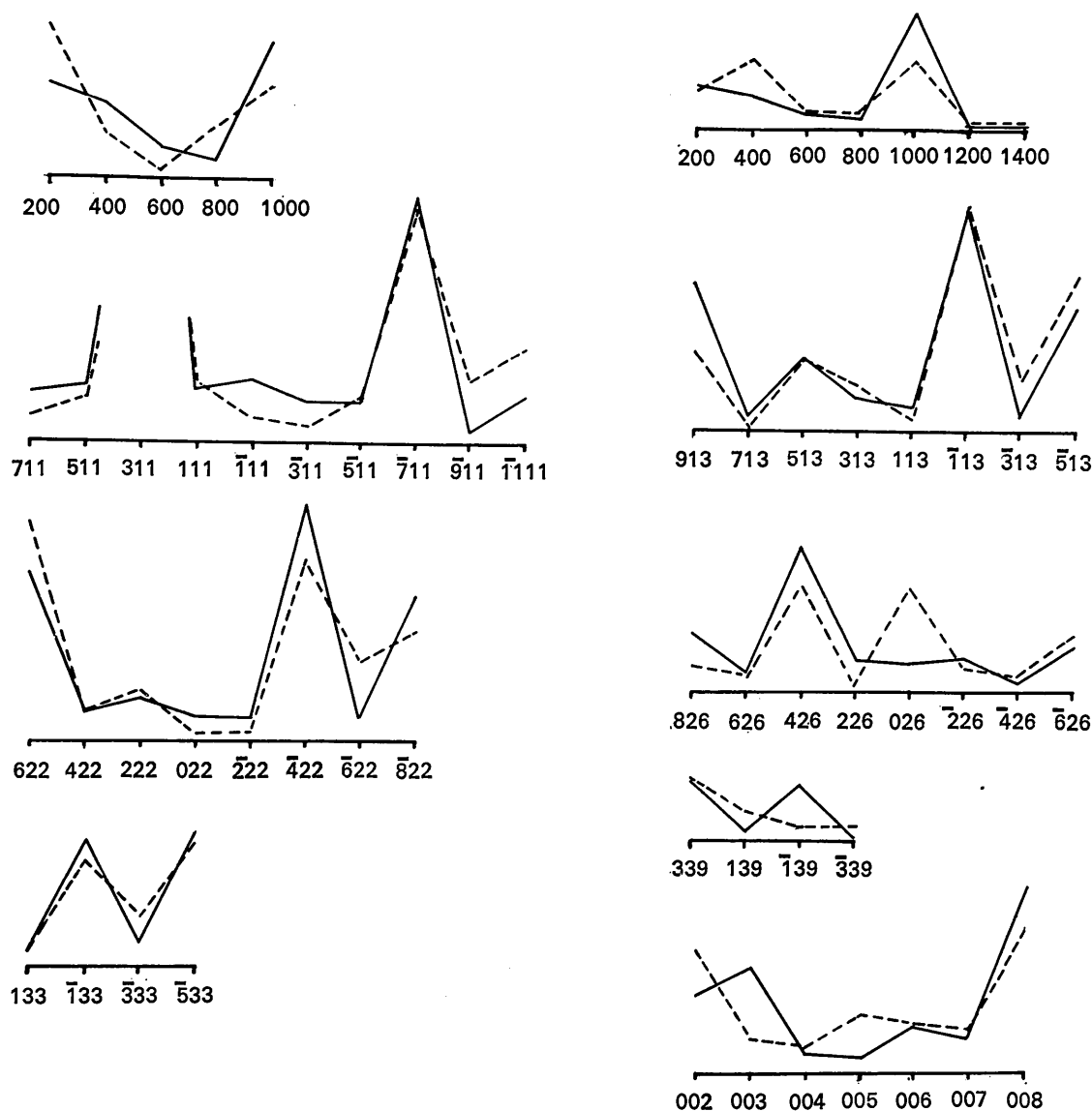


Fig. 7. Intensities calculated for the proposed structure. Correction (2) has been applied. The full lines show the observed intensities.

gation is not ideal. The origin of the diffuse scattering is not clear but an additional order of vacancies seems probable. The scattering has some of the features typical for vacancy ordering in transition-metal carbides (Sauvage & Parthé, 1972).

References

- ANDERSSON, B. & GJØNNES, J. (1970). *Acta Chem. Scand.* **24**, 2250–2252.
 ANDERSSON, B., GJØNNES, J. & TAFTØ, J. (1974). *Acta Cryst.* **A30**, 216–224.
 CAMBINI, M., PELLEGRINI, G. & AMELINCKX, S. (1971). *Mater. Res. Bull.* **6**, 791–804.
 DRITS, V. A., ORGANOVA, N. I. & DMITRIK, A. L. (1972). *Proc. Fifth European Congress on Electron Microscopy*, pp. 676–677.
 GUINIER, A. (1963). *X-ray Diffraction*. San Francisco: Freeman.
 HARADA, J. & KITAMURA, M. J. (1964). *J. Phys. Soc. Japan*, **19**, 328–343.
 ROSTOKER, W. & YAMAMOTO, A. S. (1955). *Trans. Amer. Soc. Metals*, **47**, 1002–1017.
 SAUVAGE, M. & PARTHÉ, E. (1972). *Acta Cryst.* **A28**, 607–616.
 STRINGER, J. (1965). *J. Less-Common Metals*, **8**, 1–14.
 UDALOVA, V. V. & PINSKER, Z. G. (1964). *Sov. Phys. Crystallogr.* **8**, 433–440.
 VAINSHTEIN, B. K. (1964). *Structure Analysis by Electron Diffraction*. Translated by E. FEIGL & J. A. SPINK. Oxford: Pergamon Press.

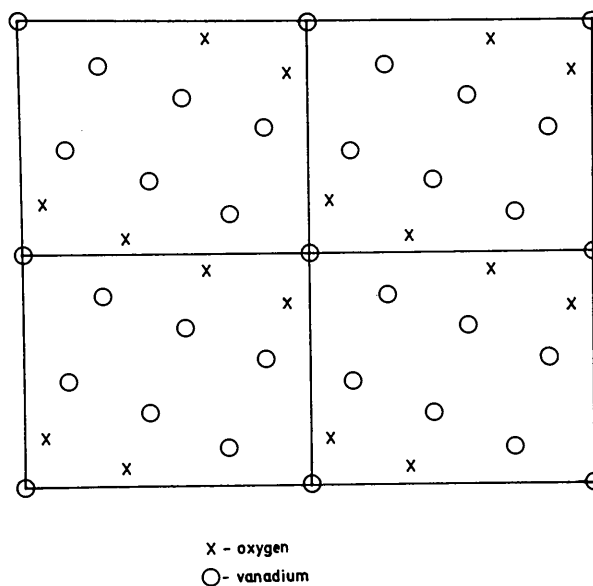


Fig. 8. The (010) plane of the proposed structure which corresponds to {110} or {100} of the NaCl and b.c.c. types of structure respectively. Full, heavy lines outline the unit cell of the γ phase.

- WESTMAN, S. (1963). *Acta Chem. Scand.* **19**, 749–752.
 WESTMAN, S. & NORDMARK, C. (1960). *Acta Chem. Scand.* **14**, 465–470.

Acta Cryst. (1975). **A31**, 70

Identification of Enantiomorphism in Crystals by Electron Microscopy

BY OMER VAN DER BIEST AND G. THOMAS

Inorganic Materials Research Division, Lawrence Berkeley Laboratory and Department of Materials Science and Engineering, College of Engineering, University of California, Berkeley, California, U.S.A.

(Received 20 June 1974; accepted 1 August 1974)

Simple electron-microscopy techniques are described which allow one to detect the presence of two enantiomorphous forms of a structure within an apparent single crystal. The first method consists of a characterization of the interface between the two enantiomorphs. In the second method advantage is taken of violations of Friedel's law which can occur in non-centrosymmetric crystals. These techniques have been illustrated by an analysis of the domain structure in ordered LiFe_3O_8 , which has a space group $P4_132$ or $P4_332$. Consistent results were obtained with both methods. The first method yields a more complete description of the domain structure. Methods which can be used to determine the absolute configuration of the structure in a part of the crystal are discussed.

1. Introduction

When a structure belongs to a space group which does not contain a symmetry operation of the second sort, that is an operation which does not involve an inversion or a reflection, then it can exist in either a right-handed or a left-handed form. In some cases these two forms have different space groups, which

are an enantiomorphous pair of space groups. With ordinary X-ray diffraction techniques it is impossible to distinguish between these two enantiomorphous forms. It is necessary to include anomalous scattering in the calculations and often very accurate intensity measurements are necessary. The use of anomalous scattering of X-rays to determine the absolute configuration of a structure has been reviewed by Rama-